

## Double-layer structure of the crust beneath the Zhongdian arc, SW China: U–Pb geochronology and Hf isotope evidence

Kang Cao <sup>a,b</sup>, Ji-Feng Xu <sup>a,c,\*</sup>, Jian-Lin Chen <sup>a,c,\*</sup>, Xiao-Xiao Huang <sup>b</sup>, Jiang-Bo Ren <sup>b</sup>, Xiang-Dong Zhao <sup>d</sup>, Zhen-Xing Liu <sup>d</sup>

<sup>a</sup> State Key Laboratory of Isotope Geochemistry, Guangzhou Institute of Geochemistry, Chinese Academy of Sciences, Guangzhou 510640, China

<sup>b</sup> University of Chinese Academy of Sciences, Beijing 100049, China

<sup>c</sup> Chinese Academy of Sciences Center for Excellence in Tibetan Plateau Earth Sciences, Beijing 100101, China

<sup>d</sup> Kunming Prospecting Design Institute of China Nonferrous Metals Industry, Kunming 650051, China



### ARTICLE INFO

#### Article history:

Received 15 January 2015

Received in revised form 28 October 2015

Accepted 30 October 2015

Available online 30 October 2015

#### Keywords:

Late Triassic porphyry

Cretaceous granite

Metallogenesis

Zhongdian arc

Double-layer crustal structure

### ABSTRACT

U–Pb ages and Hf isotopes of zircons in Late Triassic and Cretaceous intrusive rocks from the Zhongdian arc, SW China, are used to decipher the tectonic, magmatic, and metallogenic processes that occurred during this period. New U–Pb dating of zircons from Late Triassic porphyries yielded ages of ca. 216 Ma and  $\varepsilon_{\text{Hf}}(t)$  values of –2.1 to +6.1. Combined with previous results, the data indicate that these Late Triassic rocks were most likely derived from a juvenile mafic lower-crust with minor old crust material. However, the Cretaceous granites (~80 Ma) have lower  $\varepsilon_{\text{Hf}}(t)$  values (–7.6 to –2.4) than the Late Triassic rocks, indicating that the former originated from old crust. Based on the new data and previous studies of Mesozoic magmatic activity, a plausible model for the tectono-magmatism and metallogenesis of the Zhongdian arc is proposed. The westwards subduction of the Ganzi–Litang oceanic crust began before ~230 Ma, resulting in the formation of a juvenile lower crust beneath the Zhongdian arc due to the underplating of mafic arc magmas during ca. 230–216 Ma. At ca. 216 Ma, break-off or slab-tearing of the west-dipping Ganzi–Litang oceanic slab led to partial melting of the juvenile lower crust, which gave rise to Cu-bearing porphyries. In the Late Cretaceous, the Zhongdian arc probably underwent post-collision extension, triggering the partial melting of the old middle–upper crustal materials and producing various granites and related Mo–Cu deposits. According to this model, the crust beneath the Zhongdian arc probably has a double-layer structure, with older crust at shallow levels and juvenile crust at deeper levels.

© 2015 Elsevier Ltd. All rights reserved.

### 1. Introduction

The Yidun arc, part of the Sanjiang Tethyan Orogenic Belt (STOB) in southwest China, is considered to be a result of the westwards subduction of the Ganzi–Litang oceanic crust in the Late Triassic. The Zhongdian arc is the southern part of the Yidun arc, and it contains Late Triassic porphyry Cu deposits (e.g., Pulang, Xuejiping, and Chundu) (Hou et al., 2004b, 2007; Li et al., 2011; Wang et al., 2011; Chen et al., 2014) and Cretaceous Mo–Cu polymetallic deposits (e.g., Xiuwacu, Relin, and Hongshan) (Li et al., 2007, 2013; H. J. Peng et al., 2014; X. S. Wang et al., 2014a,b), as well as related granitic intrusions and volcanic rocks (Li et al.,

2007, 2013; Wang et al., 2011; H. J. Peng et al., 2014; T. P. Peng et al., 2014; X. S. Wang et al., 2014a,b).

Previous studies of Mesozoic intrusions and related deposits in this region have enhanced our understanding of the processes of subduction of the Ganzi–Litang oceanic slab and the collision of the Yidun arc and Yangtze block. However, the ages and formation mechanisms of Late Triassic ore-bearing porphyries (e.g., S. X. Wang et al., 2008a; Ren, 2011; Wang et al., 2011; Leng et al., 2012; Chen et al., 2014) and Late Cretaceous granitic intrusions related to Mo–Cu polymetallic deposits (e.g., Xu et al., 2006; Li et al., 2007, 2013; Huang, 2013; Meng et al., 2013; H. J. Peng et al., 2014; X. S. Wang et al., 2014a,b) remain debated.

In this contribution, we present new U–Pb ages and Hf isotopic compositions of zircons from Mesozoic intrusions of the Zhongdian arc, including Late Triassic ore-bearing porphyries and Late Cretaceous granites. We also present new whole-rock major and trace element compositional data for these rocks. These data, combined

\* Corresponding authors at: State Key Laboratory of Isotope Geochemistry, Guangzhou Institute of Geochemistry, Chinese Academy of Sciences, Guangzhou 510640, China.

E-mail addresses: [jifengxu@gig.ac.cn](mailto:jifengxu@gig.ac.cn) (J.-F. Xu), [lzxchen@gig.ac.cn](mailto:lzxchen@gig.ac.cn) (J.-L. Chen).

with previous results, allow us to (1) constrain the spatial and temporal distribution, and petrogenesis of Mesozoic magmatism in the Zhongdian arc; (2) evaluate the distinctive porphyry Cu mineralization in the Late Triassic Zhongdian arc compared with other regions in the wider Yidun arc; and (3) reveal the geodynamic setting and formation mechanisms of the Mesozoic magmatism and mineralization.

## 2. Geological background

The eastern Tibetan Plateau comprises three microcontinents: the Qiangtang block, the Songpan–Ganzi terrane, and the intervening NNW–SSE-trending Yidun terrane (Roger et al., 2010; Yang et al., 2012). The Yidun terrane is bound by two Paleo-Tethys sutures: the Ganzi–Litang suture to the east and the Jinshajiang suture to the west, which are related to the closure of two different Paleo-Tethys oceans during the Middle–Late Triassic and late Paleozoic, respectively (Wang et al., 2000; Reid et al., 2005; Pan et al., 2003; Pullen et al., 2008).

The Yidun terrane has been divided into the western Yidun terrane (also known as the Zhongza Massif; Wang et al., 2011) and the eastern Yidun terrane (also known as the Yidun arc; Reid et al., 2005, 2007), separated by the N–S-trending Xiangcheng–Geza fault zone (Fig. 1; BGMRSP, 1991). The oldest rocks exposed in the Zhongza Massif are Neoproterozoic granitic gneisses and metavolcanic rocks (BGMRSP, 1991). The most prevalent strata are Triassic volcanic rocks intercalated with flysch deposits (BGMRSP, 1991). The Zhongza Massif is commonly thought to have rifted from the western Yangtze block during the opening of the Ganzi–Litang ocean, triggered by the late Permian Emeishan mantle plume (Song et al., 2004; Xiao et al., 2004; Leng et al., 2012; Wang et al., 2013a; T. P. Peng et al., 2014). The Yidun arc formed at the western margin of the Yangtze craton as a result of the westwards subduction of the Ganzi–Litang oceanic crust, and it is dominated by N–S-trending Upper Triassic volcanics and sedimentary successions (BGMRSP, 1991; Li et al., 2011; Wang et al., 2011, 2013a). In addition, numerous Late Triassic to Cenozoic dioritic–granitic plutons were intruded into the Triassic volcanic and sedimentary rocks (Fig. 1; Reid et al., 2007; Weislogel, 2008; Wang et al., 2011; Chen et al., 2014).

In the northern part of the Yidun arc (the Changtai arc), a Triassic back-arc basin formed, and volcanic rocks and granitic plutons occur in two N–S trending belts (Fig. 1). Preliminary isotopic dating indicates that the volcanic rocks formed between ca. 230 and 218 Ma (Hou et al., 2004b, 2007; Wang et al., 2013b; Deng et al., 2014; Yang et al., 2014). The Zhongdian arc, which is the southern part of the Yidun arc, contains many Late Triassic intermediate–felsic porphyritic intrusions and associated andesites. The porphyries host porphyry Cu deposits, including the Pulang, Xuejiping, Chundu, and Lannitang deposits (Hou et al., 2004b, 2007; Li et al., 2011; Ren, 2011; Wang et al., 2011; Leng et al., 2012; Chen et al., 2014). In addition, several Late Cretaceous Mo–Cu polymetallic deposits related to the granitic plutons are found in this region, such as in the Xiuwacu, Relin, Hongshan, and Tongchanggou areas (Xu et al., 2006; Li et al., 2007, 2013; Meng et al., 2013; H. J. Peng et al., 2014; X. S. Wang et al., 2014a,b; Yang et al., 2015).

## 3. Samples

Samples of the Late Triassic porphyry, including quartz diorites (samples 6628–588, HS-01), quartz monzonites (samples 5618–135, XJPB, LNTY, CD-4), and granodiorites (samples 0409–303, CL-01), were collected from the Pulang, Hongshan, Lannitang, Xuejiping, Chundu, and Cilai areas. The Late Cretaceous granite samples (HS-02, 10RL-04, 10XWC-01) are from the Hongshan,

Relin, and Xiuwacu areas. All of the above samples were used for zircon U–Pb dating and Hf isotope analysis (Fig. 1b).

The Late Triassic samples have porphyritic textures, and the phenocrysts include plagioclase, K-feldspar, biotite, amphibole, and quartz. The euhedral or subhedral phenocrysts (15–30 vol.%) range in size from 1 to >10 mm across; the matrix is composed mainly of plagioclase, biotite, and quartz (<0.8 mm in size). The Late Cretaceous granites are typically coarse- to medium-grained, and contain quartz (25–40 vol.%), K-feldspar (20–25 vol.%), plagioclase (15–25 vol.%), and biotite (5–10 vol.%), as well as accessory zircon, apatite, titanite, and ilmenite.

## 4. Analytical methods and results

The analytical methods used for measuring zircon U–Pb ages, whole-rock major and trace element abundances, and *in situ* Hf isotope compositions are described in Supplementary Materials 1 (S1).

### 4.1. Zircon U–Pb ages

Nine samples were collected from the Zhongdian arc and their zircons dated (Tables 1 and S2). The zircon grains are mostly euhedral to subhedral and have long to short prismatic forms, with length-to-width ratios from 1:1 to 4:1 (Fig. 2). They are transparent, colorless<sup>1</sup> to slightly cloudy, and show oscillatory zoning indicative of magmatic growth (Fig. 2). Therefore, our interpretation of the zircon U–Pb isotopic dating results (see below) is that they represent the times the zircons crystallized, and thus the times of emplacement of the host rocks.

Samples 6628–588, 5618–135, and 0409–303 were collected from the quartz diorite, quartz monzonite, and granodiorite intrusions in the Pulang area, respectively. Their zircons yielded  $^{206}\text{Pb}/^{238}\text{U}$  weighted mean ages of  $215.5 \pm 1.6$  Ma (MSWD = 1.0),  $215.8 \pm 1.3$  Ma (MSWD = 0.1), and  $216.0 \pm 1.5$  Ma (MSWD = 0.8), respectively (Fig. 3a–c).

Sample XJPB was collected from the quartz monzonite intrusion in the Xuejiping area. Analyses of 24 zircon grains yielded a  $^{206}\text{Pb}/^{238}\text{U}$  age of  $213.4 \pm 1.5$  Ma (MSWD = 0.9) (Fig. 3d).

Sample HS-01 was collected from the quartz diorite intrusion in the Hongshan area. Ten zircon grains were analyzed, yielding a  $^{206}\text{Pb}/^{238}\text{U}$  age of  $216.4 \pm 2.7$  Ma (MSWD = 0.5) (Fig. 3e).

Sample CL-01 was collected from the granodiorite intrusion in the Cilai area. All 21 analyzed spots on 21 zircon grains fall on the concordant line within analytical error, and gave a  $^{206}\text{Pb}/^{238}\text{U}$  age of  $216.2 \pm 1.4$  Ma (MSWD = 0.1) (Fig. 3f).

Sample HS-02 was collected from the granite intrusion in the Hongshan area. Sixteen analyses on 16 different zircon grains yielded a  $^{206}\text{Pb}/^{238}\text{U}$  age of  $75.0 \pm 1.3$  Ma (MSWD = 2.2) (Fig. 3g).

Sample 10RL-04 was collected from the biotite monzogranite intrusion in the Relin area. We analyzed 16 spots on 16 different zircons, yielding a  $^{206}\text{Pb}/^{238}\text{U}$  age of  $76.8 \pm 0.8$  Ma (MSWD = 0.8) (Fig. 3h).

Sample 10XWC-01 was collected from the monzogranite intrusion in the Xiuwacu area. Sixteen analyses were carried out on 16 different zircon grains, yielding a  $^{206}\text{Pb}/^{238}\text{U}$  age of  $80.2 \pm 1.1$  Ma (MSWD = 1.4) (Fig. 3i).

### 4.2. Whole-rock geochemistry

Major and trace element concentrations are listed in Table 2 and illustrated in Figs. 5 and 6. The geochemical data obtained during

<sup>1</sup> For interpretation of color in Fig. 2, the reader is referred to the web version of this article.

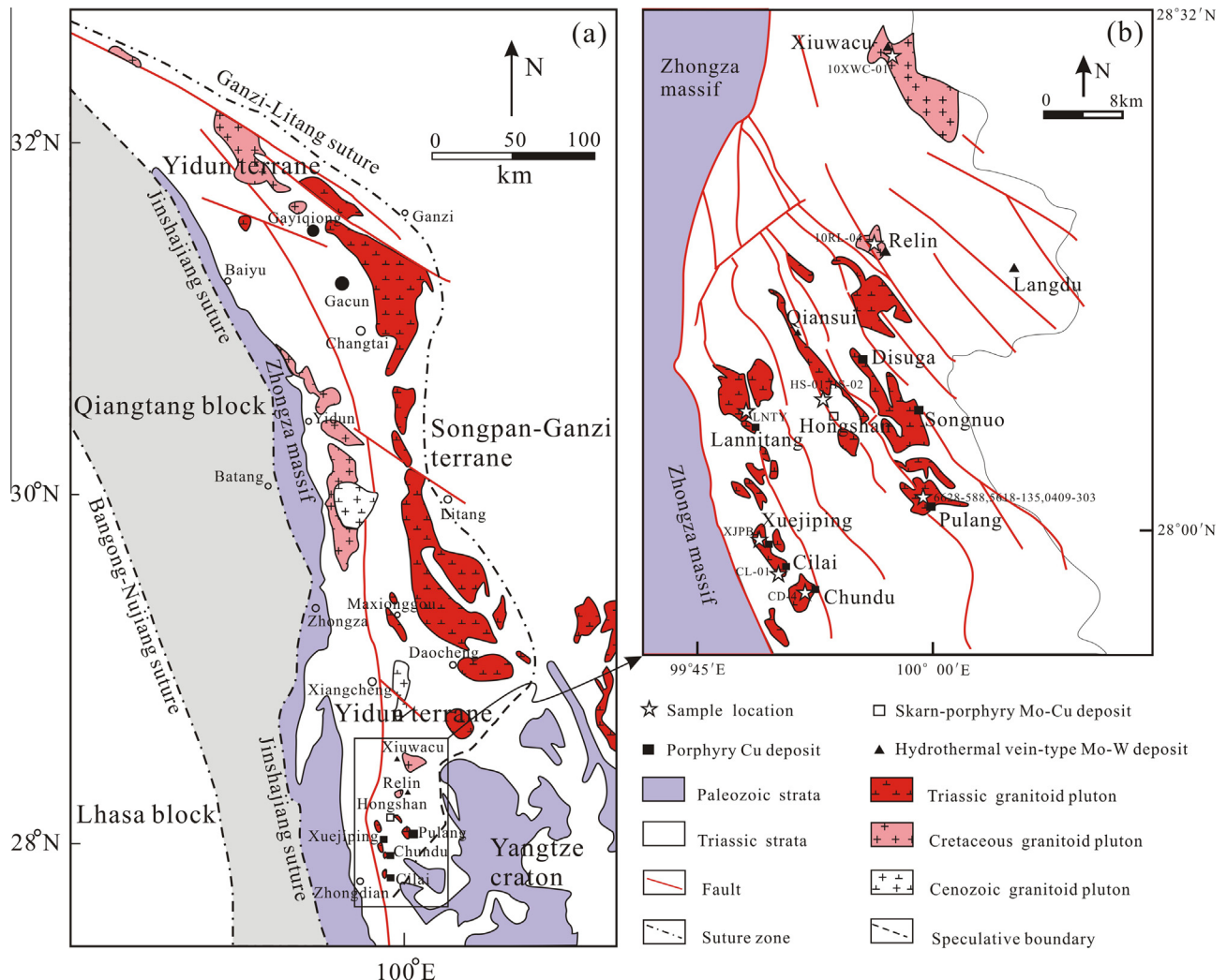


**Fig. 1.** (a) Simplified geological map of the Yidun arc (modified after X. S. Wang et al. (2014a)), and (b) sketch geological map of the Zhongdian arc belt (modified after Leng et al. (2012)).

this study, as well as previously published results for the Zhongdian arc, show that the Late Triassic porphyries have silica contents between 56.6 and 68.3 wt.% and total alkali contents of 3.1–9.6 wt.% (Ren, 2011; Wang et al., 2011; Huang, 2013; Chen et al., 2014; Table 2). These porphyries can be broadly grouped as quartz monzonite and monzonite (Fig. 4a). In contrast, the Late Cretaceous granites mainly plot in the field of granites, with SiO<sub>2</sub> contents of 68.3–76.0 wt.% (except for a few samples in the field of quartz monzonite, Fig. 4a). On the SiO<sub>2</sub> versus K<sub>2</sub>O diagram, the porphyries and the granites mostly plot in the high-K calc-alkaline to shoshonite fields (Fig. 4b). The Late Triassic porphyries have relatively high contents of MgO (1.7–4.2 wt.%, average 3.1 wt.%) and Al<sub>2</sub>O<sub>3</sub> (13.8–16.7 wt.%, average 15.1 wt.%), and K<sub>2</sub>O/Na<sub>2</sub>O ratios that are mostly >1.2 (Ren, 2011; Huang, 2013; Chen et al., 2014; Table 2), whereas the Late Cretaceous granites have relatively low contents of MgO (<1.1 wt.%) and Al<sub>2</sub>O<sub>3</sub> (12.5–15.0 wt.%, average 13.5 wt.%), and K<sub>2</sub>O/Na<sub>2</sub>O ratios that are mostly >1.3 (Huang, 2013; X. S. Wang et al., 2014a,b; Table 2).

The two sets of rocks both exhibit sub-parallel chondrite-normalized rare earth elements (REE) patterns, characterized by clear fractionation between light REEs (LREEs) and heavy REEs (HREEs). However, compared with the Late Triassic porphyries, the Late Cretaceous granites have significant Eu anomalies

(Eu/Eu\* = 0.26–0.69) (Fig. 5a and c). In primitive-mantle-normalized spider diagrams (Fig. 5b and d), the Late Triassic porphyries are enriched in large ion lithophile elements (LILEs; e.g., Rb, Ba, and Th) and depleted in high field strength elements (HFSEs), with prominent negative anomalies in Nb-Ta and Ti. In addition, they have high Sr (258–1115 ppm) and low Y (11–19 ppm) concentrations, with high Sr/Y ratios (18–97). Compared with the Late Triassic porphyries, the Late Cretaceous granites have low Ba and Sr contents, and high Rb and Th contents; they also have Sr/Y ratios of 2–22.

#### 4.3. Zircon Hf isotope compositions

Zircon Hf isotopes were analyzed for all the zircon grains from the above nine analyzed samples and the other two samples (LNTY and CD-4; Chen et al., 2014). Given that these samples have concordant or nearly concordant U-Pb ages, their Hf isotope compositions can be taken to indicate the origin of the parental melt (Stille and Steiger, 1991).

##### 4.3.1. Late Triassic porphyries

Zircons from the Late Triassic porphyries have <sup>176</sup>Hf/<sup>177</sup>Hf isotope ratios ranging from 0.282585 to 0.282821, and the average

**Table 1**

Representative LA-ICP-MS U-Pb data for zircons from the Triassic porphyries and Cretaceous granites in the Zhongdian arc (see Table S2 in supplementary materials for the complete dataset).

Spot	Th ppm	U ppm	Th/U	$^{207}\text{Pb}/^{235}\text{U}$		$^{206}\text{Pb}/^{238}\text{U}$		$^{207}\text{Pb}/^{206}\text{Pb}$		$^{207}\text{Pb}/^{235}\text{U}$		$^{206}\text{Pb}/^{238}\text{U}$	
				Ratio	1 $\sigma$	Ratio	1 $\sigma$	Age	1 $\sigma$	Age	1 $\sigma$	Age	1 $\sigma$
<i>Sample XJPB, Locality: 28°00'39"N, 99°48'37"E</i>													
XJPB-01	474	518	0.92	0.23699	0.01832	0.03378	0.00059	237	172	216	15	214	4
XJPB-02	413	508	0.81	0.24145	0.01694	0.03435	0.00056	241	157	220	14	218	4
XJPB-03	423	599	0.71	0.23701	0.01945	0.03392	0.00065	228	183	216	16	215	4
XJPB-04	588	600	0.98	0.2343	0.01852	0.03366	0.00062	219	177	214	15	213	4
XJPB-05	919	891	1.03	0.24585	0.01509	0.03397	0.00054	308	137	223	12	215	3
XJPB-06	557	652	0.85	0.23439	0.01525	0.03419	0.00053	184	148	214	13	217	3
XJPB-07	425	531	0.80	0.26908	0.02194	0.03438	0.00069	483	175	242	18	218	4
XJPB-08	829	830	1.00	0.27363	0.01626	0.03341	0.00054	583	127	246	13	212	3
XJPB-09	534	596	0.90	0.24483	0.02059	0.03299	0.00068	365	184	222	17	209	4
XJPB-10	688	710	0.97	0.24811	0.01675	0.03391	0.00058	333	149	225	14	215	4
XJPB-11	1167	1008	1.16	0.25746	0.01459	0.03344	0.00051	447	125	233	12	212	3
<i>Sample HS-02, Locality: 28°07'24"N, 99°53'27"E</i>													
HS-02-01	878	1363	0.64	0.07923	0.00601	0.01164	0.00028	150	172	77	6	75	2
HS-02-02	414	955	0.43	0.07120	0.00524	0.01158	0.00022	–	–	70	5	74	1
HS-02-03	149	481	0.31	0.08312	0.01064	0.01272	0.00037	165	285	81	10	81	2
HS-02-04	568	794	0.72	0.07280	0.00605	0.01162	0.00029	–	–	71	6	74	2
HS-02-05	668	2083	0.32	0.07116	0.00503	0.01159	0.00032	–	–	70	5	74	2
HS-02-06	433	1054	0.41	0.06899	0.00560	0.01155	0.00028	–	–	68	5	74	2
HS-02-07	420	1164	0.36	0.08118	0.00614	0.01170	0.00025	209	187	79	6	75	2
HS-02-08	371	1069	0.35	0.08754	0.00668	0.01185	0.00025	383	188	85	6	76	2
HS-02-09	563	1193	0.47	0.06877	0.00654	0.01161	0.00037	–	–	68	6	74	2
HS-02-10	606	1328	0.46	0.08355	0.00732	0.01197	0.00031	217	200	81	7	77	2
HS-02-11	775	1333	0.58	0.08207	0.00670	0.01167	0.00030	206	–5	80	6	75	2

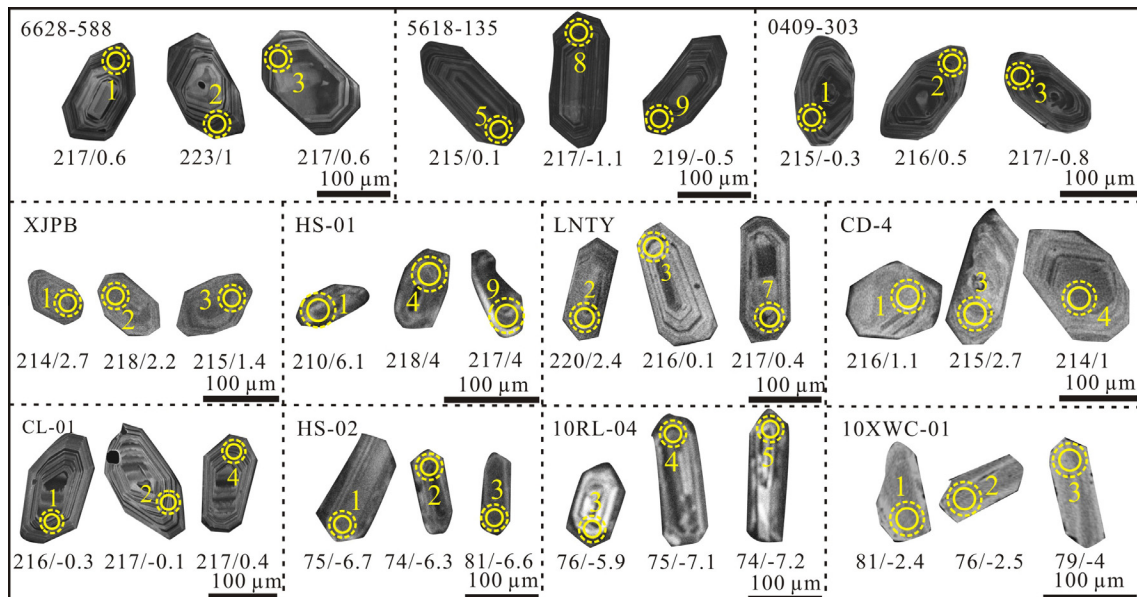


**Fig. 2.** Representative cathodoluminescence (CL) images of selective zircons from the Late Triassic porphyries and Cretaceous granites of the Zhongdian arc. Solid circles show U-Pb analysis spots, and dashed circles Hf analysis spots. The numbers correspond to the analyses in Tables S2 and S3.

$\varepsilon_{\text{Hf}}(t)$  values for the eight samples range from  $-2.1 \pm 0.7$  to  $+6.1 \pm 1.4$ , yielding two-stage Hf model ages of 1233–773 Ma (Tables 3 and S3; Fig. 6).

#### 4.3.2. Late Cretaceous granites

Zircons from the Late Cretaceous granites have  $^{176}\text{Hf}/^{177}\text{Hf}$  isotopic ratios ranging from 0.282510 to 0.282655, and the average  $\varepsilon_{\text{Hf}}(t)$  values for the three samples range from  $-7.6 \pm 0.6$  to  $-2.4 \pm 0.8$ , yielding two-stage Hf model ages of 1434–1147 Ma (Tables 3 and S3; Fig. 6).

## 5. Discussion

### 5.1. Geochronology

#### 5.1.1. Late Triassic magmatism in the Zhongdian arc

Previous studies of the Late Triassic igneous rocks in the Yidun arc seemed to indicate that the rocks are related to the westwards subduction of the Ganzi–Litang oceanic crust (Chen et al., 2014). Zircon U-Pb dating of the volcanic sequences in the entire Yidun arc indicates that they developed from ca. 230 to ca. 213 Ma

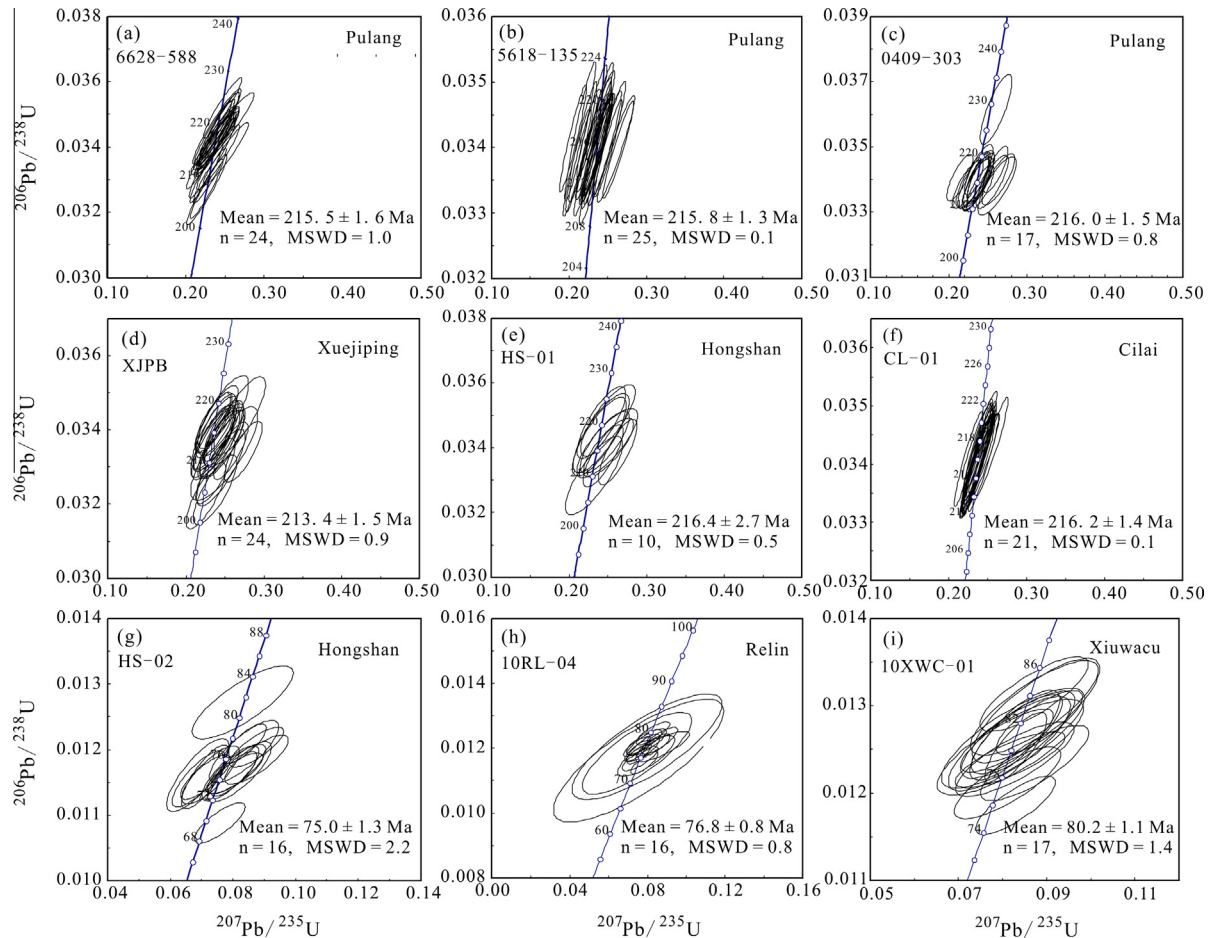


**Fig. 3.** U-Pb concordia diagrams for zircons from the following rocks of the Late Triassic and Cretaceous: (a) quartz diorite, (b) quartz monzonite, and (c) granodiorite from the Pulang area; (d) quartz monzonite from the Xuejiping area; (e) quartz diorite from the Hongshan area; and (f) granodiorite from the Cilai area; (g) granite from the Hongshan area; (h) biotite monzogranite from the Relin area; and (i) monzogranite from the Xiuwacu area.

(e.g., Huang, 2013; Wang et al., 2013b; Leng et al., 2014; Yang et al., 2014). In the Zhongdian arc, local porphyritic rocks (e.g., Pulang, Xuejiping, Chundu, and Hongshan) are spatially associated with volcanic rocks. The available U-Pb ages for zircons from the porphyries are variable, ranging from 230 to 206 Ma, even for a given porphyry in a given deposit (Table 4). Our new systematic U-Pb dating of zircons from the Zhongdian arc porphyries, combined with existing data, demonstrates that all of the porphyries formed at ca. 216 Ma. Accordingly, the emplacement of the porphyries was initiated about 14 Myr after the earliest volcanic activity in the Yidun arc, and this volcanic activity may represent the westwards subduction of the Ganzi-Litang oceanic crust in the Late Triassic (Wang et al., 2013b).

#### 5.1.2. Late Cretaceous magmatism in the Zhongdian arc

The Yidun arc was probably subjected to post-collisional extension during the period from 189 to 73 Ma, and corresponding magmatic activity developed in both the Changtai and Zhongdian arcs (Hou et al., 2004b; Yang et al., 2002). Nevertheless, preliminary geochronological studies, mainly using whole-rock Rb-Sr and biotite Ar-Ar dating, constrain the timing of emplacement of the Cretaceous granites in the Zhongdian arc (e.g., Yin et al., 2009; Li et al., 2013; and references therein). However, considering these rocks have undergone extensive hydrothermal alteration (e.g., Li et al., 2007), the results of Rb-Sr and Ar-Ar dating are suspect, because these isotope systems are likely to have been affected by such alteration. In contrast, zircon is a robust mineral and resistant to

any late-stage hydrothermal alteration. This means that the U-Pb isotopic system would have remained closed and retained its suitability for dating. Recent and ongoing studies of the Cretaceous granites and the related Mo-Cu polymetallic deposits in the Zhongdian arc have now provided high-quality zircon U-Pb ages (e.g., H. J. Peng et al., 2014; X. S. Wang et al., 2014a).

Our new zircon U-Pb ages suggest that the granitic intrusions in the Hongshan Cu-Mo polymetallic deposit, the Relin Mo-W-Cu deposit, and the Xiuwacu Mo-W deposit were formed at  $75.0 \pm 1.3$  Ma,  $76.8 \pm 0.8$  Ma, and  $80.2 \pm 1.1$  Ma, respectively. The U-Pb ages are within error of molybdenite Re-Os ages obtained for these deposits (ca. 83–76 Ma) (Li et al., 2007, 2011; Zu et al., 2015). Therefore, Late Cretaceous magmatism and mineralization in the Zhongdian arc took place synchronously during post-collisional extension.

#### 5.2. Petrogenesis

##### 5.2.1. Late Triassic porphyries

Major and trace element data for the Late Triassic ore-related porphyries from the Zhongdian arc show adakitic affinities (Fig. 7; Ren, 2011; Wang et al., 2011; Chen et al., 2014; Table 2). Wang et al. (2011) proposed that these adakitic rocks are closely related to interactions between melts of the subducting basaltic oceanic crust and the overlying mantle wedge. However, Leng et al. (2012) considered that these rocks originated from a metasomatized mantle with 5–10% crustal contamination. Furthermore,

**Table 2**

Major and trace element data of Late Triassic porphyries and Cretaceous granites in the Zhongdian arc.

Sample	6628-588	6628-597	0406-462	XJP-3	HS-01	LNTA	CD-4	HS-02	10RL-08	10RL-09	10XWC-02	10XWC-03
Location	Pulang			Xuejiping	Hongshan	Lannitang	Chundu	Hongshan	Relin	Relin	Xiuwacu	Xiuwacu
SiO <sub>2</sub>	63.18	64.44	65.85	63.70	58.90	58.60	59.82	71.59	70.22	71.40	73.88	74.58
TiO <sub>2</sub>	0.63	0.57	0.49	0.80	1.00	1.40	0.85	0.43	0.57	0.50	0.20	0.19
Al <sub>2</sub> O <sub>3</sub>	14.27	13.96	15.69	14.10	15.64	14.90	13.76	14.16	13.93	13.79	13.55	13.25
Fe <sub>2</sub> O <sub>3</sub>	5.37	4.84	3.26	4.37	6.49	7.30	4.80	1.71	3.34	2.95	1.76	1.70
MgO	2.73	2.47	1.74	2.10	3.45	2.70	2.28	0.61	1.05	0.86	0.30	0.27
MnO	0.06	0.06	0.05	0.06	0.10	0.10	0.20	0.02	0.06	0.06	0.04	0.03
CaO	4.08	3.81	3.60	2.25	3.15	4.50	4.78	0.36	1.82	1.59	0.77	0.84
Na <sub>2</sub> O	2.60	2.82	3.92	3.51	3.66	4.00	1.86	1.38	3.09	3.21	3.49	3.52
K <sub>2</sub> O	5.34	5.43	3.46	2.74	5.48	2.30	3.56	6.99	4.25	4.36	5.23	4.88
P <sub>2</sub> O <sub>5</sub>	0.41	0.36	0.18	0.23	0.32	0.20	0.30	0.20	0.23	0.19	0.06	0.05
LOI	0.84	0.73	1.25	5.90	1.31	3.50	7.76	2.13	0.97	0.63	0.25	0.23
TOTAL	99.50	99.50	99.48	99.77	99.50	99.52	99.98	99.57	99.53	99.53	99.53	92.92
Na <sub>2</sub> O + K <sub>2</sub> O	7.94	8.25	7.38	6.25	9.14	6.30	5.42	8.37	7.34	7.57	8.72	8.39
Mg <sup>#</sup>	50.4	50.5	51.6	49.0	51.5	42.5	48.7	41.6	38.6	36.8	25.4	24.2
Sc	13.8	13.1	6.9	9.9	12.3	19.2	10.8	1.8	8.4	8.0	6.2	6.2
V	109	99	65	119	109	201	130	18	57	45	31	33
Cr	47	43	18	88	37	17	46	10	129	114	148	169
Co	7.5	8.4	7.2	9.4	13.3	17.1	8.6	6.6	6.5	6.1	2.0	1.8
Ni	14.0	14.6	11.4	11.6	15.1	16.8	11.8	4.3	10.4	9.7	5.8	6.2
Rb	178	162	93	80	271	53	146	475	186	233	421	438
Sr	796	760	1040	772	1004	1115	255	123	326	237	101	79
Y	13.8	15.1	10.7	13.8	16.7	18.7	14.6	9.3	14.7	15.6	28.4	33.8
Zr	191	337	187	134	200	199	176	227	274	203	139	160
Nb	12.4	12.7	10.9	15.5	17.9	17.9	17.0	33.9	35.4	41.5	67.1	81.0
Ba	1612	1370	1131	2124	3920	2082	2788	640	637	539	339	199
La	29.3	32.0	35.6	46.2	44.6	48.8	50.3	53.8	46.5	45.8	37.8	38.0
Ce	58.7	63.7	66.7	80.1	85.3	88.3	88.3	97.3	84.2	83.1	70.2	70.4
Pr	7.17	7.82	7.55	8.50	9.50	9.82	9.65	9.90	8.80	8.70	7.61	7.60
Nd	27.2	29.1	26.0	28.6	35.2	33.8	32.6	33.2	28.8	28.7	24.1	24.1
Sm	5.29	5.76	4.26	4.96	6.10	5.86	5.62	4.80	4.70	4.80	4.63	4.96
Eu	1.39	1.44	1.11	1.05	1.10	1.43	1.12	0.75	1.00	0.92	0.50	0.41
Gd	3.97	4.25	3.02	3.62	4.79	4.61	4.18	3.01	4.16	4.23	4.21	4.53
Tb	0.55	0.60	0.42	0.48	0.62	0.65	0.56	0.40	0.55	0.57	0.68	0.78
Dy	3.05	3.42	2.41	2.58	3.56	3.61	2.90	2.02	2.70	2.90	4.11	4.88
Ho	0.58	0.66	0.47	0.48	0.68	0.68	0.53	0.37	0.50	0.52	0.86	1.04
Er	1.55	1.83	1.34	1.34	1.83	1.76	1.40	0.90	1.42	1.46	2.62	3.20
Tm	0.23	0.28	0.19	0.19	0.26	0.25	0.20	0.13	0.22	0.22	0.46	0.55
Yb	1.48	1.76	1.30	1.29	1.59	1.61	1.26	0.85	1.37	1.51	3.25	3.83
Lu	0.23	0.29	0.21	0.20	0.24	0.23	0.20	0.13	0.22	0.24	0.53	0.59
Hf	5.13	8.50	4.86	4.08	4.84	5.08	5.29	5.41	7.15	5.73	5.08	6.02
Ta	1.02	1.18	0.87	1.25	1.25	1.21	1.29	2.45	2.82	3.92	12.13	12.50
Pb	16.3	36.3	15.3	11.1	14.3	24.4	45.7	18.9	20.2	22.3	28.1	26.2
Th	16.8	19.8	12.5	20.1	15.0	12.5	19.9	29.0	31.7	35.3	49.3	50.7
U	4.32	4.94	3.15	5.06	3.32	3.03	4.84	8.00	8.70	8.31	15.62	24.46
Sr/Y	57.7	50.3	97.2	55.8	60.1	59.6	17.5	13.2	22.2	15.2	3.6	2.3

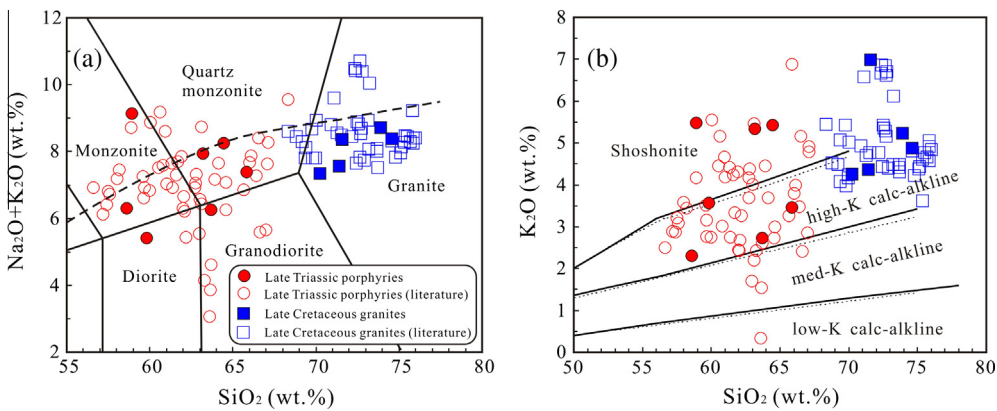


**Fig. 4.** Geochemical characteristics of the Late Triassic porphyries and Late Cretaceous granites in the Zhongdian arc. (a) Total alkali versus SiO<sub>2</sub> diagram (based on Middlemost, 1994); (b) K<sub>2</sub>O versus SiO<sub>2</sub> diagram (based on Rickwood, 1989). Data sources: Ren (2011), Wang et al. (2011), Huang (2013), Chen et al. (2014), X. S. Wang et al. (2014a,b), and this study.

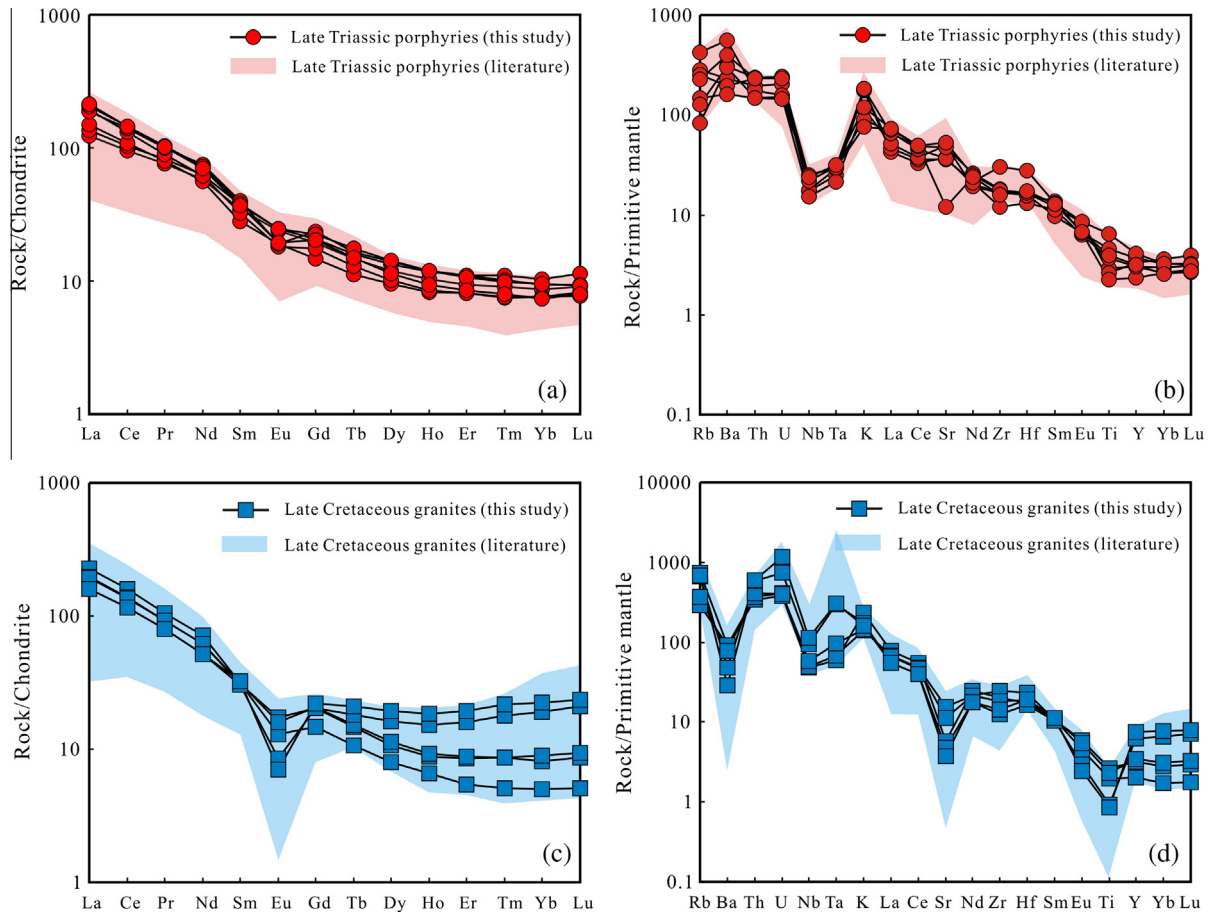


**Fig. 5.** Chondrite-normalized REE and primitive mantle-normalized trace elemental spider diagrams for the Late Triassic and Late Cretaceous granites in the Zhongdian arc. Normalizing values are from Sun and McDonough (1989). Data sources are as in Fig. 4.

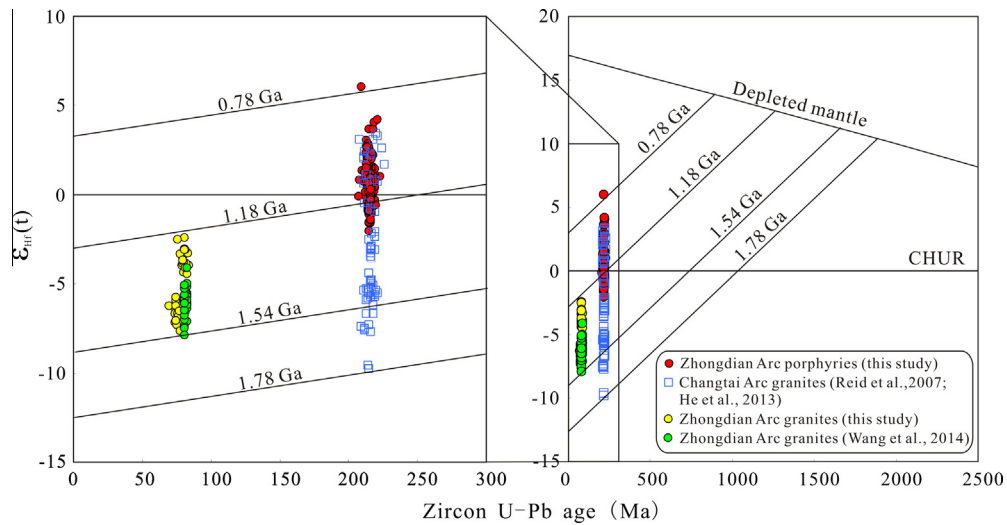


**Fig. 6.** Relationship between  $\varepsilon_{\text{Hf}}(t)$  values and U-Pb ages for zircons from the Late Triassic porphyries and Cretaceous granites of the Zhongdian arc.

Chen et al. (2014) proposed that these porphyries were produced by partial melting of a metasomatized mantle wedge that had been heated by an ascending asthenosphere due to slab break-off or slab-tearing.

Generally, the Late Triassic porphyries possess high SiO<sub>2</sub> contents (up to 68 wt.%), are potassic in nature (K<sub>2</sub>O/Na<sub>2</sub>O > 1; Wang et al., 2011; Chen et al., 2014), and show slightly negative  $\varepsilon_{\text{Nd}}$

values. Some of the porphyries have negative  $\varepsilon_{\text{Hf}}(t)$  values along with relatively high  $^{87}\text{Sr}/^{86}\text{Sr}_i$  values (Fig. 8; Wang et al., 2011; Leng et al., 2012; Cao, 2014; Chen et al., 2014). The above characteristics are clearly distinguishable from slab-derived melts (e.g., Na-rich,  $\varepsilon_{\text{Nd}}(t) > 4$ ; Stern and Kilian, 1996) and direct partial melting of the mantle (Jahn and Zhang, 1984). In addition, the Late Triassic porphyries have Th concentrations (11.4–23.6 ppm) and

**Table 3**

Representative Hf isotope data for zircons from the Triassic porphyries and Cretaceous granites in the Zhongdian arc (see Table S3 in supplementary materials for the complete dataset).

Spot	$^{176}\text{Hf}/^{177}\text{Hf}$	$1\sigma$	$^{176}\text{Lu}/^{177}\text{Hf}$	$1\sigma$	$^{176}\text{Yb}/^{177}\text{Hf}$	$1\sigma$	$t_{206/208}$ (Ma)	$\varepsilon_{\text{Hf}}(t)$	$1\sigma$	$T_{\text{DM1}}$ (Ma)	$T_{\text{DM2}}$ (Ga)
<i>Sample XJPB, Locality: 28°00'39"N, 99°48'37"E</i>											
XJPB-01	0.282718	0.000019	0.000844	0.000013	0.023396	0.000286	214	2.7	0.8	753	969
XJPB-02	0.282703	0.000016	0.000892	0.000017	0.023035	0.000406	218	2.2	0.8	776	998
XJPB-03	0.282681	0.000013	0.000932	0.000020	0.022630	0.000703	215	1.4	0.7	807	1043
XJPB-04	0.282700	0.000020	0.000754	0.000027	0.018190	0.000627	213	2.0	0.9	777	1005
XJPB-05	0.282713	0.000021	0.000911	0.000010	0.024294	0.000314	215	2.5	0.9	762	980
XJPB-06	0.282703	0.000016	0.000804	0.000013	0.022245	0.000398	217	2.2	0.8	773	997
XJPB-10	0.282745	0.000017	0.000821	0.000018	0.020094	0.000390	215	3.7	0.8	715	915
XJPB-12	0.282730	0.000024	0.000943	0.000011	0.027021	0.000381	213	3.1	1.0	739	947
XJPB-13	0.282725	0.000030	0.001308	0.000019	0.033281	0.000510	214	2.8	1.2	753	960
XJPB-14	0.282697	0.000016	0.000954	0.000014	0.024595	0.000369	217	2.0	0.8	786	1011
<i>Sample HS-02, Locality: 28°07'24"N, 99°53'27"E</i>											
HS-02-01	0.282537	0.000011	0.000847	0.000014	0.025179	0.000556	75	-6.7	0.7	1008	1381
HS-02-02	0.282550	0.000013	0.000916	0.000015	0.027052	0.000411	74	-6.3	0.7	990	1355
HS-02-03	0.282537	0.000009	0.000546	0.000037	0.016043	0.001215	81	-6.6	0.6	1000	1378
HS-02-04	0.282542	0.000011	0.000769	0.000025	0.022935	0.000984	74	-6.5	0.7	998	1371
HS-02-05	0.282547	0.000010	0.000853	0.000011	0.023301	0.000333	74	-6.4	0.6	994	1362
HS-02-06	0.282538	0.000009	0.000633	0.000025	0.017848	0.000862	74	-6.7	0.6	1000	1378
HS-02-07	0.282520	0.000011	0.000875	0.000021	0.025512	0.000825	75	-7.3	0.6	1032	1414
HS-02-08	0.282538	0.000012	0.000730	0.000018	0.022500	0.000849	76	-6.7	0.7	1003	1379
HS-02-09	0.282560	0.000011	0.001244	0.000028	0.038246	0.001040	74	-5.9	0.7	986	1338
HS-02-10	0.282532	0.000012	0.001037	0.000016	0.030698	0.000529	77	-6.8	0.7	1019	1390

**Table 4**

Summary of zircon U-Pb dating results for Late Triassic porphyries in the Zhongdian arc.

Region	Lithology	Methodology	Age (Ma)	Source
Pulang	Quartz monzonite	SHRIMP	228.3–226.0	S. X. Wang et al. (2008a)
	Quartz diorite	TIMS	221.0 ± 1.0	Pang et al. (2009)
	Quartz monzonite	TIMS	211.8 ± 0.5	Pang et al. (2009)
	Granodiorite	TIMS	206.3 ± 1.7	Pang et al. (2009)
	Quartz diorite	LA-ICP-MS	224.2–217.9	Wang et al. (2011)
	Quartz diorite	LA-ICP-MS	217.2–211.8	Chen et al. (2014)
	Quartz monzonite	LA-ICP-MS	215.3 ± 2.3	Lin et al. (2006)
Xuejiping	Quartz diorite	SHRIMP	215.2 ± 1.9	Cao et al. (2009)
	Quartz diorite	LA-ICP-MS	217.9 ± 1.8	Wang et al. (2011)
	Quartz monzonite	SIMS	218.3 ± 1.6	Leng et al. (2012)
	Quartz monzonite	LA-ICP-MS	215.9 ± 1.4	Chen et al. (2014)
	Dioritic porphyry	LA-ICP-MS	216.9–214.7	T. P. Peng et al. (2014)
	Quartz monzonite	LA-ICP-MS	216.7 ± 1.2	Chen et al. (2014)
	Quartz monzonite	SIMS	219.7 ± 1.8	Zhang et al. (2009)
Lannitang	Diorite	LA-ICP-MS	212.0 ± 3.0	Yang et al. (2011)
	Granodiorite	LA-ICP-MS	218.0–217.0	Yang et al. (2011)
	Quartz monzonite	LA-ICP-MS	215.3–213.1	Chen et al. (2014)
Songnuo	Quartz monzonite	SHRIMP	220.9 ± 3.5	Leng et al. (2008)
Qiansui	Quartz diorite	LA-ICP-MS	217.5 ± 1.5	Ren (2011)

Th/Ce ratios (0.14–0.67) (Fig. 7c and d; Ren, 2011; Wang et al., 2011; Huang, 2013; Chen et al., 2014; this study) that are higher than those of subducted oceanic crust-derived adakites, indicating that these porphyries originated from a crustal source (Hawkesworth et al., 1997; Rapp et al., 2002; Chung et al., 2003; Hou et al., 2004a, 2013a,b; Bissig and Tosdal, 2009).

The Late Triassic porphyries have geochemical features that are similar to those of the intermediate-acid adakitic batholiths in the Cordillera Blanca (Peru), which are attributed to lower-crust melting in an arc setting (Atherton and Petford, 1993; Petford and Atherton, 1996). In addition, most of the porphyries in the Zhongdian arc with low ( $^{87}\text{Sr}/^{86}\text{Sr}$ ) ratios and relatively high  $\varepsilon_{\text{Nd}}(t)$  values partly overlap the fields of the adakitic porphyries of the Tibetan collisional zone (Hou et al., 2004a) and of the Cordillera Blanca (Petford and Atherton, 1996), both of which are suggested to have been derived from a juvenile mafic lower crust involving mantle components via underplating of mantle-derived mafic magmas (Atherton and Petford, 1993; Hou et al., 2004a, 2013a). Furthermore, the  $\varepsilon_{\text{Hf}}(t)$  values of zircons from the Late Triassic porphyries of the present study range from -2.1 to +6.1, which are obviously different from those of contemporaneous granites in the Changtai arc and the Late Cretaceous granites in the Zhongdian arc, both of which originated from an old crustal source (Fig. 6; Reid et al., 2007; He et al., 2013; see the following discussion). Collectively, the above geochemical features and Sr-Nd-Hf isotopic compositions indicate that the Late Triassic porphyries were derived from a common juvenile lower continental crust (Hou et al., 2004a, 2009, 2013a,b; Wang et al., 2006; Xiao et al., 2007), with the addition of small amounts of old crustal material.

### 5.2.2. Late Cretaceous granites

The petrogenesis of the Late Cretaceous granites associated with the Mo-Cu polymetallic deposits in the Zhongdian arc remains debated, and several genetic models have been proposed: (1) partial melting of the middle-lower crust (Huang, 2013); (2) derivation of the adakitic rocks mainly from a thickened lower continental crust (X. S. Wang et al., 2014a); and (3) re-melting of a residual oceanic slab (H. J. Peng et al., 2014).

Our new geochemical data show that the Late Cretaceous granites have high contents of  $\text{SiO}_2$  (>70 wt.%) and  $\text{K}_2\text{O}$  ( $\text{K}_2\text{O}/\text{Na}_2\text{O} > 1$ ), low contents of  $\text{MgO}$  (<1.1 wt.%) and  $\text{Sr}$  (mostly <300 ppm), and relatively low  $\text{Sr/Y}$  ratios (1–22; average 9). These geochemical features, combined with the low concentrations of compatible elements (e.g.,  $\text{V} = 18$ –57 ppm,  $\text{Co} = 1.8$ –6.6 ppm, and  $\text{Ni} = 4.3$ –10.4 ppm) and the highly fractionated REE patterns (Fig. 5c), strongly suggest a crustal source rather than a mantle origin. In

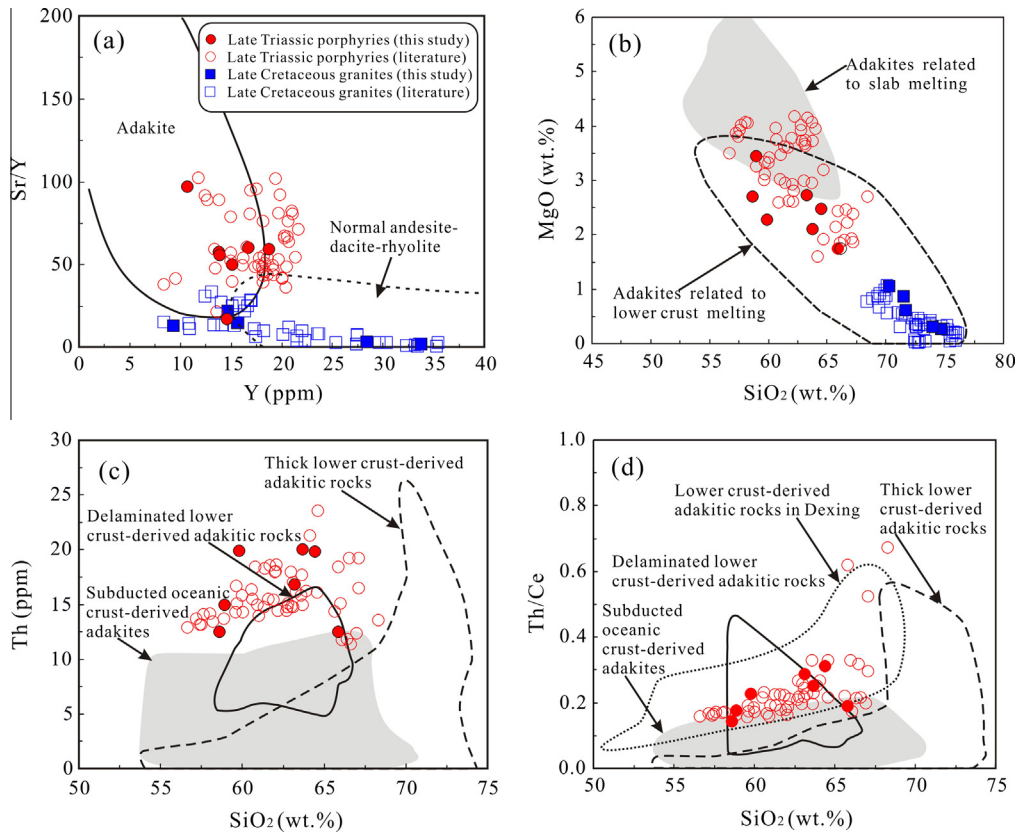


**Fig. 7.** (a) Plots of  $\text{Sr}/\text{Y}$  vs.  $\text{Y}$  (after Drummond and Defant (1990)); (b)  $\text{MgO}$  vs.  $\text{SiO}_2$  diagram (after Hou et al. (2013a)); (c)  $\text{Th}$  vs.  $\text{SiO}_2$  diagram (after Wang et al. (2006)); (d)  $\text{Th}/\text{Ce}$  vs.  $\text{SiO}_2$  diagram (after Wang et al. (2006)). Data sources: Dexing adakitic rocks from Hou et al. (2013a), others are as in Fig. 4.

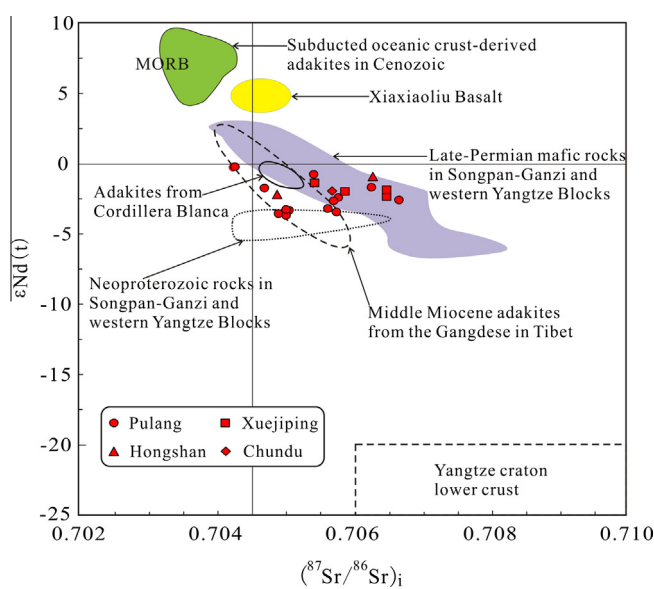


**Fig. 8.** Diagram of  $(^{87}\text{Sr}/^{86}\text{Sr})_i$  vs.  $\varepsilon_{\text{Nd}}(t)$  for the Late Triassic porphyries in the Zhongdian arc. Data sources: Pulang porphyries from Cao (2014); Xuejiping porphyries from Wang et al. (2011) and Chen et al. (2014); Hongshan porphyries from Huang (2013); Chundu porphyries from Chen et al. (2014); Xiaoxiaoliu basalt from Ren (2011); Cordillera Blanca adakitic intrusions from Petford and Atherton (1996); adakitic intrusions of the Gangdese porphyry Cu belt in Tibet from Hou et al. (2004a, 2013b); oceanic slab-derived adakites from Kay (1978), Kay and Kay (1993), and Stern and Kilian (1996); late Permian mafic rocks from the Songpan-Ganzi and western Yangtze blocks from Q. Wang et al. (2008); Neoproterozoic igneous and metamorphic rocks from the Songpan-Ganzi and western Yangtze blocks from Roger and Calassou (1997) and Li et al. (2003); and Yangtze Craton lower crust field from Li et al. (2009).

addition, the granites have negative  $\varepsilon_{\text{Nd}}(t)$  values ( $-7.7$  to  $-2.8$ ; Huang, 2013; Meng, 2014), and the Hf isotope compositions of zircons we studied show  $\varepsilon_{\text{Hf}}(t)$  values ranging from  $-7.6$  to  $-2.4$ , even lower than those of coeval granites ( $-3.9$  to  $\sim 0.0$ ) in the Changtai arc, which are interpreted to have been derived by partial melting of old crust (Reid et al., 2007). We suggest, therefore, that the Late Cretaceous granites were derived from an old continental crustal source.

### 5.3. Geodynamic setting

It is generally accepted that the evolutionary history of the Yidun arc has involved Late Triassic subduction of oceanic crust (ca. 238–210 Ma), Late Triassic–Early Jurassic arc–continent collision (ca. 207–189 Ma), Jurassic–Cretaceous post-collisional extension (ca. 189–73 Ma), and finally Tertiary intra-continental strike-slip shearing (ca. 65–15 Ma) (Qu et al., 2003; Hu et al., 2005; Zhao et al., 2007). However, in the Late Triassic, different tectonic frameworks and rock assemblages existed in the northern and southern parts of the Yidun arc, due to differences in the slab subduction angle (steep in the north and shallow in the south; Hou et al., 2004b, 2007). Correspondingly, a back-arc basin and bimodal volcanic suites were developed in the northern part (i.e., the Changtai arc), while normal arc magmatic rocks (e.g., andesites and felsic porphyries) and associated porphyry copper deposits (e.g., at Pulang) were developed in the southern part (i.e., the Zhongdian arc).

The arc volcanic rocks that formed in the Changtai arc at ca. 230 Ma indicate that the westwards subduction of the Ganzi–Litang oceanic crust had already started in the early Late Triassic (Wang et al., 2013b). Meanwhile, the Late Triassic porphyries in the Zhongdian arc were formed during a transient

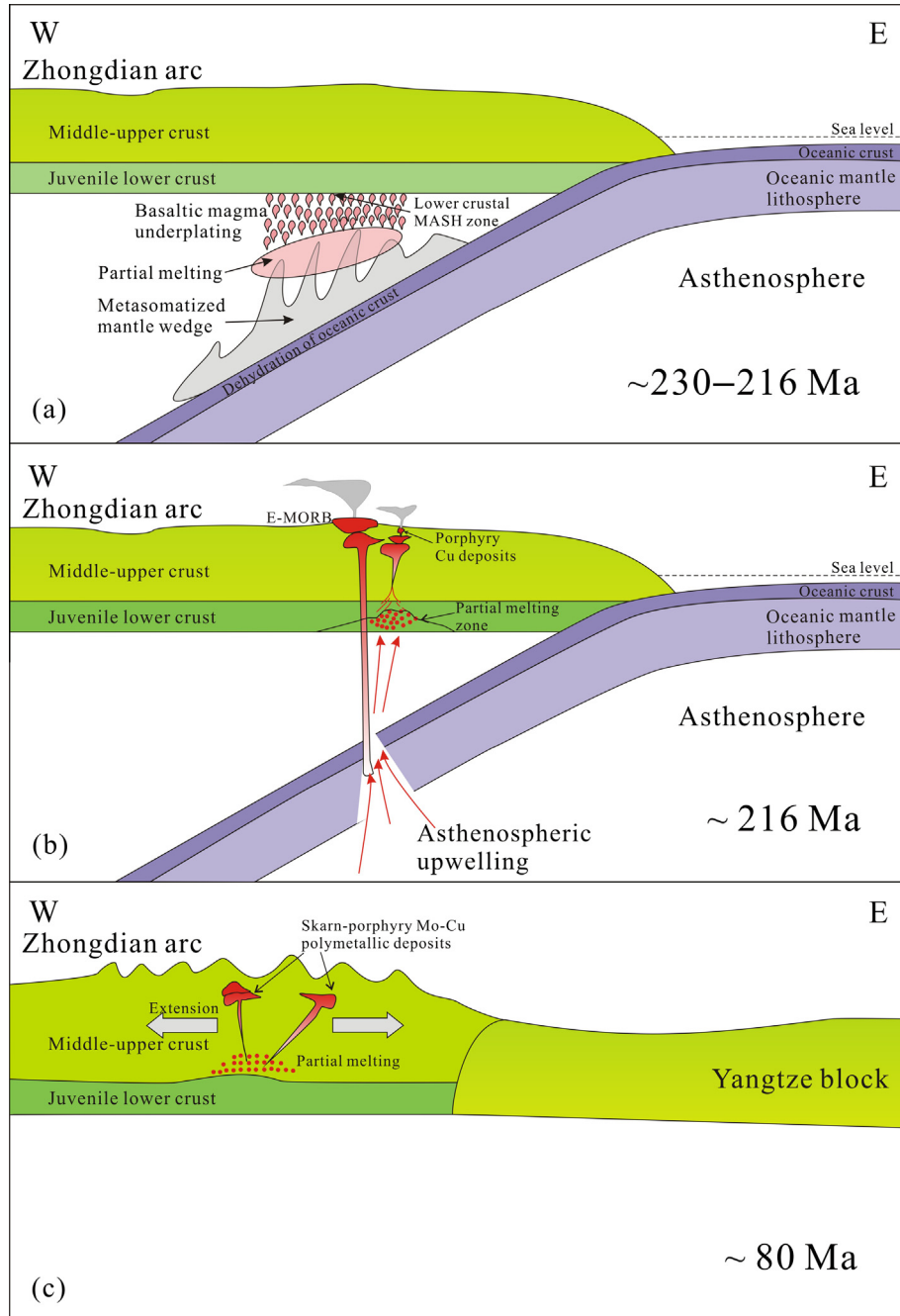


**Fig. 9.** Proposed model for the tectono-magmatism and metallogenesis of the Zhongdian arc.

period with a concentration of ages at ca. 216 Ma, which is similar to the ages of andesites in the same region (ca. 219–213 Ma; Huang, 2013; Leng et al., 2014). Therefore, the time of formation of the porphyries postdates by about 14 Myr the initiation of the arc volcanic activity in the Changtai arc. Based on the discussion above, we propose a two-stage tectonomagmatic model for the formation of the porphyries in the Zhongdian arc (in present coordinates). In the first stage (Fig. 9a; ca. 230–216 Ma), the westwards subduction of the Ganzi-Litang oceanic lithosphere led to partial melting of the metasomatized mantle wedge and subsequent underplating of arc basaltic magmas to form a juvenile lower crust at the crust-mantle boundary or in the MASH zone (Richards, 2003) beneath the Zhongdian arc. In the second stage (Fig. 9b;

ca. 216 Ma), anatexis of the juvenile lower crust was induced by upwelling of the asthenosphere (probably caused by slab break-off or slab-tearing), and this led to the formation of the adakitic porphyries in the Zhongdian arc. This interpretation is consistent with the identification of coeval E-MORB basalts in the Xiaxiaoliu area (Ren, 2011).

The ages of Late Cretaceous granites and Mo-Cu deposits in the Zhongdian arc (ca. 83–76 Ma) overlap with those of the northern Yidun arc granites (116 to ca. 76 Ma), which are considered to have formed in an intra-continental extensional setting (Reid et al., 2007, and references therein). On the basis of this regional intra-continental extensional tectonic model, Huang (2013) suggested that the Late Cretaceous granites are related to the delamination

of the lithospheric mantle during the arc–continent collision stage. However, post-collisional extension took place during the Early Jurassic in the Yidun arc (X. S. Wang et al., 2014a), as intraplate felsic volcanic rocks and A-type granites formed in both the Songpan–Ganzi terrane and the Yidun arc at 189–182 Ma (Qu et al., 2003; Hu et al., 2005; Zhao et al., 2007). Furthermore, there is no evidence that delamination of the lithosphere occurred in the Zhongdian arc during the Late Cretaceous (evidence such as widespread Late Cretaceous basalt magmatism). Although the dynamic mechanism causing the intraplate extension remains unknown and requires further study, the negative Hf isotopic compositions of the Late Cretaceous granites indicate that they were derived from an old crustal source, which suggests in turn that an old crust existed in the study area (Fig. 9c).

If the above interpretation is correct, then it indicates that there is a double-layer structure of the crust beneath the Zhongdian arc, with juvenile crust at low levels and older crust at middle–upper levels.

#### 5.4. Implications for mineralization

A prerequisite for the formation of an arc porphyry Cu system is considered to be the generation of hydrous and sulfur-rich calc-alkaline basaltic arc magmas with a high  $fO_2$  (Richards, 2003). Such magmas originate from an enriched mantle wedge metasomatized by fluids derived from a subducted slab. Subsequently, the mafic magmas underplate the lower crust, undergoing a MASH process to form evolved, volatile-rich, and metalliferous intermediate to felsic magmas (Richards, 2003). In the Late Triassic, the entire Yidun arc formed due to the westwards subduction of the Ganzi–Litang oceanic lithosphere. Porphyry Cu deposits occur only in the southern part of the arc (i.e., the Zhongdian arc). This limited distribution of metallogenesis is inferred to reflect differences in the magma sources. Unlike normal arc magmas, the Cu-bearing porphyries in the Zhongdian arc are potassic, relatively oxidized, and adakitic, and they were derived from a juvenile lower crust formed by underplating of former arc basaltic magmas, as discussed above. Re-melting and remobilization of underplated mafic material (including sulfide-bearing metal-rich cumulates at the base of the crust that formed during the earlier arc magmatism) probably provided the Cu, Au, and S for the porphyry Cu systems (Richards, 2009; Lee et al., 2012; R. Wang et al., 2014; Hou et al., 2015). In addition, the pervasive biotite phenocrysts and hydrothermal alteration of the ore-bearing porphyries in the Zhongdian arc indicate high magmatic water contents (~4 wt.%), which is also a critical factor in the generation of porphyry Cu deposits (Richards, 2003, 2009; Hou et al., 2009, 2013a). The high  $H_2O$  content of these porphyries can probably be attributed to the melting of  $H_2O$ -bearing amphibolite cumulates that were the residues of underplated arc magmas, and which then saw the breakdown of hornblende, thus releasing  $H_2O$  (Richards, 2009). Metal-rich cumulates in the early-stage juvenile crust probably contributed to the enrichment of ore-forming elements (Lee et al., 2012), and subsequently the slab break-off or slab-tearing may have provided enough heat to fuse the juvenile lower crust. Thus, in the Zhongdian arc area, conditions were optimal for the formation of porphyry copper systems, in contrast to other parts of the Yidun arc. Hence, the key factors that controlled the Cu mineralization in the study area are likely to have been the juvenile lower crust and slab break-off or slab-tearing.

In the Late Cretaceous, Mo–Cu polymetallic deposits developed in the Zhongdian arc. Magmas derived from old crustal materials, with minor contributions from the mantle, would have supplied Mo, W, and other metal elements, as reported for the Qinling porphyry Cu deposits (Hou and Yang, 2009). In addition, the S isotopes of the sulfides in the Mo–Cu polymetallic deposits of

the Zhongdian arc provide support for a crustal source for these sulfides (S. X. Wang et al., 2008b; Li et al., 2013).

#### 6. Conclusions

- (1) The Late Triassic porphyries in the Zhongdian arc were formed mainly at ca. 216 Ma, postdating by about 14 Myr the eruption of the earliest volcanic rocks in the Yidun arc as a whole. The Late Cretaceous post-collisional granites in the Zhongdian arc were generally emplaced at ca. 80 Ma.
- (2) The Late Triassic porphyries and Late Cretaceous granites in the Zhongdian arc were derived mainly from a juvenile lower crust and an older middle–upper crust, respectively.
- (3) The interplay of two key factors, namely the double-layer structure of the crust and the process of slab break-off or slab-tearing, most likely led to the metallogenic system of the Zhongdian arc, which is distinct from metallogenic systems in other regions of the Yidun arc.

#### Acknowledgements

This research was supported by the following funding agencies: the Major State Basic Research Program of the People's Republic of China (2015CB452602), the Strategic Priority Research Program (B) of the Chinese Academy of Sciences (XDB03010300), the China Geology Survey project (1212011220908), the Natural Science Foundation of China (41373030, 41573024), and the GIGCAS 135 project of the Guangzhou Institute of Geochemistry (Y234021002). Constructive comments and suggestions by Associated Editor J.G. Liou and two anonymous reviewers helped to improve the manuscript. This is GIGCAS contribution No. IS-2156.

#### Appendix A. Supplementary material

Supplementary data associated with this article can be found, in the online version, at <http://dx.doi.org/10.1016/j.jseaes.2015.10.024>.

#### References

- Atherton, M.P., Petford, N., 1993. Generation of sodium-rich magmas from newly underplated basaltic crust. *Nature* 362, 144–146.
- BGMRSP (Bureau of Geology and Mineral Resources of Sichuan Province), 1991. Regional Geology of Sichuan Province. Geological Publishing House, Beijing, 730 pp (in Chinese with English abstract).
- Bissig, T., Tosdal, R.M., 2009. Petrogenetic and metallogenic relationships in the Eastern Cordillera Occidental of Central Peru. *J. Geol.* 117, 499–518.
- Cao, K., 2014. Tectono–magmatism–metallogenesis of Zhongdian arc and the mineralization of the giant Pulang porphyry copper deposit. MD Thesis of University of Chinese Academy of Sciences, 122pp (in Chinese with English abstract).
- Cao, D.H., Wang, A.J., Li, W.C., Wang, G.S., Li, R.P., Li, Y.K., 2009. Magma mixing in the Pulang porphyry copper deposit: evidence from petrology and element geochemistry. *Acta Geol. Sin.* 83, 166–175 (in Chinese with English abstract).
- Chen, J.L., Xu, J.F., Ren, J.B., Huang, X.X., Wang, B.D., 2014. Geochronology and geochemical characteristics of Late Triassic porphyritic rocks from the Zhongdian arc, eastern Tibet, and their tectonic and metallogenic implications. *Gondwana Res.*, 492–504.
- Chung, S.L., Liu, D., Ji, J., Chu, M.F., Lee, H.Y., Wen, D.J., Lo, C.H., Lee, T.Y., Qian, Q., Zhang, Q., 2003. Adakites from continental collision zones: melting of thickened lower crust beneath southern Tibet. *Geology* 31, 1021–1024.
- Deng, J., Wang, Q.F., Li, G.J., Li, C.S., Wang, C.M., 2014. Tethys tectonic evolution and its bearing on the distribution of important mineral deposits in the Sanjiang region, SW China. *Gondwana Res.* 26, 419–437.
- Drummond, M.S., Defant, M.J., 1990. A model for trondhjemite–tonalite–dacite genesis and crustal growth via slab melting: Archean to modern comparisons. *J. Geophys. Res.* 95, 21503–21521.
- Hawkesworth, C., Turner, S., McDermott, F., Peate, D., Van Calsteren, P., 1997. U–Th isotopes in arc magmas: implications for element transfer from the subducted crust. *Science* 276, 551–555.
- He, D.F., Zhu, W.G., Zhong, H., Ren, T., Bai, Z.J., Fan, H.P., 2013. Zircon U–Pb geochronology and elemental and Sr–Nd–Hf isotopic geochemistry of the

- Daocheng granitic pluton from the Yidun Arc, SW China. *J. Asian Earth Sci.* 67, 1–17.
- Hou, Z.Q., Yang, Z.M., 2009. Porphyry deposits in continental settings of China: geological characteristics, magmatic-hydrothermal system, and metallogenetic model. *Acta Geol. Sin.* 83, 1779–1817 (in Chinese with English abstract).
- Hou, Z.Q., Gao, Y.F., Qu, X.M., Rui, Z.Y., Mo, X.X., 2004a. Origin of adakitic intrusives generated during mid-Miocene east–west extension in southern Tibet. *Earth Planet. Sci. Lett.* 220, 139–155.
- Hou, Z.Q., Yang, Y.Q., Qu, X.M., Huang, D.H., Lv, Q.T., Wang, H.P., Yu, J.J., Tang, S.H., 2004b. Tectonic evolution and mineralization systems of the Yidun arc orogen in Sanjiang region, China. *Acta Geol. Sin.* 78, 109–120 (in Chinese with English abstract).
- Hou, Z.Q., Zaw, K., Pan, G.T., Mo, X.X., Xu, Q., Hu, Y.Z., Li, X.Z., 2007. Sanjiang Tethyan metallogenesis in SW China: tectonic setting, metallogenetic epochs and deposit types. *Ore Geol. Rev.* 31, 48–87.
- Hou, Z.Q., Yang, Z.M., Qu, X.M., Meng, X.J., Li, Z.Q., Beaudoin, G., Rui, Z.Y., Gao, Y.F., Zaw, K., 2009. The Miocene Gangdese porphyry copper belt generated during post-collisional extension in the Tibetan Orogen. *Ore Geol. Rev.* 36, 25–51.
- Hou, Z.Q., Pan, X.F., Li, Q.Y., Yang, Z.M., Song, Y.C., 2013a. The giant Dexing porphyry Cu–Mo–Au deposit in east China: product of melting of juvenile lower crust in an intracontinental setting. *Miner. Deposita* 48, 1019–1045.
- Hou, Z.Q., Zheng, Y.C., Yang, Z.M., Rui, Z.Y., Zhao, Z.D., Jiang, S.H., Qu, X.M., Sun, Q.Z., 2013b. Contribution of mantle components within juvenile lower crust to collisional zone porphyry Cu systems in Tibet. *Miner. Deposita* 48, 173–192.
- Hou, Z.Q., Yang, Z.M., Lu, Y.J., Kemp, Anthony, Zheng, Y.C., Li, Q.Y., Tang, J.X., Yang, Z.S., Duan, L.F., 2015. A genetic linkage between subduction- and collision-related porphyry Cu deposits in continental collision zones. *Geology* 43, 247–250.
- Hu, J.M., Meng, Q.R., Shi, Y.R., Qu, H.J., 2005. SHRIMP U–Pb dating of zircons from granitoid bodies in the Songpan–Ganzi terrane and its implications. *Acta Petrol. Sin.* 21, 867–880 (in Chinese with English abstract).
- Huang, X.X., 2013. Geochronology, geochemistry and petrogenesis of Indosinian and Yanshanian igneous rocks in Zhongdian arc. MD Thesis of University of Chinese Academy of Sciences, 82pp (in Chinese with English abstract).
- Jahn, B.M., Zhang, Z.Q., 1984. Archean granulite gneisses from eastern Hebei Province, China: rare earth geochemistry and tectonic implications. *Contrib. Miner. Petrol.* 85, 224–243.
- Kay, R., 1978. Aleutian magnesian andesites: melts from subducted Pacific Ocean crust. *J. Volcanol. Geoth. Res.* 4, 117–132.
- Kay, R.W., Kay, S.M., 1993. Delamination and delamination magmatism. *Tectonophysics* 219, 177–189.
- Lee, C.T.A., Luffi, P., Chin, E.J., Bouchet, R., Dasgupta, R., Morton, D.M., Jin, D., 2012. Copper systematics in arc magmas and implications for crust–mantle differentiation. *Science* 336, 64–68.
- Leng, C.B., Zhang, X.C., Wang, S.X., Qin, C.J., Gou, T.Z., Wang, W.Q., 2008. SHRIMP zircon U–Pb dating of the Songnuo ore-hosted porphyry, Zhongdian, northwest Yunnan, China and its geological implication. *Geotect. Metall.* 32, 124–130 (in Chinese with English abstract).
- Leng, C.B., Zhang, X.C., Hu, R.Z., Wang, S.X., Zhong, H., Wang, W.Q., Bi, X.W., 2012. Zircon U–Pb and molybdenite Re–Os geochronology and Sr–Nd–Pb–Hf isotopic constraints on the genesis of the Xuejipings porphyry copper deposit in Zhongdian, Northwest Yunnan, China. *J. Asian Earth Sci.* 60, 31–48.
- Leng, C.B., Huang, Q.Y., Zhang, X.C., Wang, S.X., Zhong, H., Hu, R.Z., Bi, X.W., Zhu, J.J., Wang, X.S., 2014. Petrogenesis of the Late Triassic volcanic rocks in the Southern Yidun arc, SW China: constraints from the geochronology, geochemistry, and Sr–Nd–Pb–Hf isotopes. *Lithos* 190–191, 363–382.
- Li, Z.X., Li, X.H., Kinny, P.D., Wang, J., Zhang, S., Zhou, H., 2003. Geochronology of neoproterozoic syn-rift magmatism in the Yangtze Craton, South China and correlations with other continents: evidence for a mantle superplume that broke up Rodinia. *Precambrian Res.* 122, 85–109.
- Li, J.K., Li, W.C., Wang, D.H., Lu, Y.X., Yin, G.H., Xue, S.R., 2007. Re–Os dating for ore-forming event in the late of Yanshan Epoch and research of ore-forming regularity in Zhongdian Arc. *Acta Petrol. Sin.* 23, 2415–2422 (in Chinese with English abstract).
- Li, J.W., Zhao, X.F., Zhou, M.F., Ma, C.Q., De Souza, Z.S., Vasconcelos, P., 2009. Late Mesozoic magmatism from the Daye region, eastern China: U–Pb ages, petrogenesis, and geodynamic implications. *Contrib. Miner. Petrol.* 157, 383–409.
- Li, W.C., Zeng, P.S., Hou, Z.Q., White, N.C., 2011. The Pulang porphyry copper deposit and associated felsic intrusions in Yunnan Province, Southwest China. *Econ. Geol.* 106, 79–92.
- Li, W.C., Yu, H.J., Yin, G.H., 2013. Porphyry metallogenic system of Geza arc in the Sanjiang region, southwestern China. *Acta Petrol. Sin.* 29, 1129–1144 (in Chinese with English abstract).
- Lin, Q.C., Xia, B., Zhang, Y.Q., 2006. Zircon SHRIMP U–Pb dating of the syn-collisional Xuejipings quartz diorite porphyrite in Zhongdian, Yunnan, China, and its geological implications. *Geol. Bull. China* 25, 133–135 (in Chinese with English abstract).
- Meng, J.Y., 2014. The porphyry copper–polymetallic deposit in Zhongdian, west Yunnan: magmatism and mineralization. DD Thesis of China University of Geosciences, 197pp (in Chinese with English abstract).
- Meng, J.Y., Yang, L.Q., Lv, L., Gao, X., Li, J.X., Luo, Y.Z., 2013. Re–Os dating of molybdenite from the Hongshan Cu–Mo deposit in Northwest Yunnan and its implications for mineralization. *Acta Petrol. Sin.* 29, 1214–1222 (in Chinese with English abstract).
- Middlemost, E.A.K., 1994. Naming materials in the magma/igneous rock system. *Earth Sci. Rev.* 37, 215–224.
- Pan, G.T., Xu, Q., Hou, Z.Q., Wang, L.Q., Du, D.X., Mo, X.X., Li, D.M., Wang, M.J., Li, X.Z., Jiang, X.S., 2003. Archipelagic Orogenesis, Metallogenic Systems and Assessment of the Mineral Resources along the Nujiang–Lancangjiang–Jinshajiang Area in Southwestern China. Geological Publishing House, Beijing, 420 pp (in Chinese with English abstract).
- Pang, Z.S., Du, Y.S., Wang, G.W., Guo, X., Cao, Y., Li, Q., 2009. Single-grain zircon U–Pb isotopic ages, geochemistry and implication of the Pulang complex in Yunnan Province, China. *Acta Petrol. Sin.* 25, 159–165 (in Chinese with English abstract).
- Peng, H.J., Mao, J.W., Pei, R.F., Zhang, C.Q., Tian, G., Zhou, Y.M., Li, J.X., Hou, L., 2014. Geochronology of the Hongniu–Hongshan porphyry and skarn Cu deposit, northwestern Yunnan province, China: implications for mineralization of the Zhongdian arc. *J. Asian Earth Sci.* 79, 682–695.
- Peng, T.P., Zhao, G.C., Fan, W.M., Peng, B.X., Mao, Y.S., 2014. Zircon geochronology and Hf isotopes of Mesozoic intrusive rocks from the Yidun terrane, Eastern Tibetan Plateau: petrogenesis and their bearings with Cu mineralization. *J. Asian Earth Sci.* 80, 18–33.
- Petford, N., Atherton, M., 1996. Na-rich partial melts from newly underplated basaltic crust: the Cordillera Blanca Batholith, Peru. *J. Petrol.* 37, 1491–1521.
- Pullen, A., Kapp, P., Gehrels, G.E., Vervoort, J.D., Ding, L., 2008. Triassic continental subduction in central Tibet and Mediterranean-style closure of the Paleo-Tethys Ocean. *Geology* 36, 351–354.
- Qu, X.M., Hou, Z.Q., Tang, S.H., 2003. Age of intraplate volcanism in the back-arc area of Yidun island arc and its significance. *Acta Petrol. Mineral.* 22, 131–137 (in Chinese with English abstract).
- Rapp, R.P., Xiao, L., Shimizu, N., 2002. Experimental constraints on the origin of potassium-rich adakites in eastern China. *Acta Petrol. Sin.* 18, 293–302.
- Reid, A.J., Wilson, C.J., Liu, S., 2005. Structural evidence for the Permo-Triassic tectonic evolution of the Yidun Arc, eastern Tibetan Plateau. *J. Struct. Geol.* 27, 119–137.
- Reid, A., Wilson, C.J., Shun, L., Pearson, N., Belousova, E., 2007. Mesozoic plutons of the Yidun Arc, SW China: U/Pb geochronology and Hf isotopic signature. *Ore Geol. Rev.* 31, 88–106.
- Ren, J.B., 2011. The chronology, geochemistry and mineralization significance of porphyry copper deposits in Zhongdian Island Arc. MD Thesis of Graduate School of Chinese Academy of Sciences, 82pp (in Chinese with English abstract).
- Richards, J.P., 2003. Tectono-magmatic precursors for porphyry Cu–(Mo–Au) deposit formation. *Econ. Geol.* 98, 1515–1533.
- Richards, J.P., 2009. Postsubduction porphyry Cu–Au and epithermal Au deposits: products of remelting of subduction-modified lithosphere. *Geology* 37, 247–250.
- Rickwood, P.C., 1989. Boundary lines within petrologic diagrams which use oxides of major and minor elements. *Lithos* 22, 247–263.
- Roger, F., Calassou, S., 1997. U–Pb geochronology on zircon and isotopic geochemistry (Pb, Sr and Nd) of the basement in the Songpan–Garze fold belt (China). *C. R. Acad. Sci., IIA, Earth Planet. Sci.* 324, 819–826.
- Roger, F., Jolivet, M., Malavieille, J., 2010. The tectonic evolution of the Songpan–Garze (North Tibet) and adjacent areas from Proterozoic to Present: a synthesis. *J. Asian Earth Sci.* 39, 254–269.
- Song, X.Y., Zhou, M.F., Cao, Z.M., Robinson, P.T., 2004. Late Permian rifting of the South China Craton caused by the Emeishan mantle plume? *J. Geol. Soc.* 161, 773–781.
- Stern, C.R., Kilian, R., 1996. Role of the subducted slab, mantle wedge and continental crust in the generation of adakites from the Andean Austral Volcanic Zone. *Contrib. Miner. Petrol.* 123, 263–281.
- Stille, P., Steiger, R.H., 1991. Hf isotope systematics in granitoids from the central and southern Alps. *Contrib. Miner. Petrol.* 107, 273–278.
- Sun, S.S., McDonough, W.F., 1989. Chemical and isotopic systematics of oceanic basalts: implications for mantle composition and processes. *Geol. Soc., London, Spec. Publ.* 42, 313–345.
- Wang, X.F., Metcalfe, I., Jian, P., He, L.Q., Wang, C.S., 2000. The Jinshajiang–Ailaoshan suture zone, China: tectonostratigraphy, age and evolution. *J. Asian Earth Sci.* 18, 675–690.
- Wang, Q., Xu, J.F., Jian, P., Bao, Z.W., Zhao, Z.H., Li, C.F., Xiong, X.L., Ma, J.L., 2006. Petrogenesis of adakitic porphyries in an extensional tectonic setting, Dexing, South China: implications for the genesis of porphyry copper mineralization. *J. Petrol.* 47, 119–144.
- Wang, S.X., Zhang, X.C., Leng, C.B., Qin, C.J., Ma, D.Y., Wang, W.Q., 2008a. Zircon SHRIMP U–Pb dating of the Pulang porphyry copper deposit, northwestern Yunnan, China: the ore-forming time limitation and geological significance. *Acta Petrol. Sin.* 24, 2313–2321 (in Chinese with English abstract).
- Wang, S.X., Zhang, X.C., Leng, C.B., Qin, C.J., Wang, W.Q., Zhao, M.X., 2008b. Stable isotopic compositions of the Hongshan skarn copper deposit in the Zhongdian area and its implication for the copper mineralization process. *Acta Petrol. Sin.* 24, 480–488 (in Chinese with English abstract).
- Wang, Q., Wyman, D.A., Xu, J.F., Dong, Y.H., Vasconcelos, P.M., Pearson, N., Wan, Y.S., Dong, H., Li, C.F., Yu, Y.S., Zhu, T.X., Feng, X.T., Zhang, Q.Y., Zi, F., Chu, Z.Y., 2008. Eocene melting of subducting continental crust and early uplifting of central Tibet: evidence from central–western Qiangtang high-K calc-alkaline andesites, dacites and rhyolites. *Earth Planet. Sci. Lett.* 272, 158–171.
- Wang, B.Q., Zhou, M.F., Li, J.W., Yan, D.P., 2011. Late Triassic porphyritic intrusions and associated volcanic rocks from the Shangri-La region, Yidun terrane, Eastern Tibetan Plateau: adakitic magmatism and porphyry copper mineralization. *Lithos* 127, 24–38.
- Wang, B.Q., Wang, W., Chen, W.T., Gao, J.F., Zhao, X.F., Yan, D.P., Zhou, M.F., 2013a. Constraints of detrital zircon U–Pb ages and Hf isotopes on the provenance of the Triassic Yidun Group and tectonic evolution of the Yidun Terrane, Eastern Tibet. *Sed. Geol.* 289, 74–98.

- Wang, B.Q., Zhou, M.F., Chen, W.T., Gao, J.F., Yan, D.P., 2013b. Petrogenesis and tectonic implications of the Triassic volcanic rocks in the northern Yidun Terrane, Eastern Tibet. *Lithos* 175, 285–301.
- Wang, X.S., Bi, X.W., Leng, C.B., Zhong, H., Tang, H.F., Chen, Y.W., Yin, G.H., Huang, D.Z., Zhou, M.F., 2014a. Geochronology and geochemistry of Late Cretaceous igneous intrusions and Mo–Cu–(W) mineralization in the southern Yidun Arc, SW China: implications for metallogenesis and geodynamic setting. *Ore Geol. Rev.* 61, 73–95.
- Wang, X.S., Hu, R.Z., Bi, X.W., Leng, C.B., Pan, L.C., Zhu, J.J., Chen, Y.W., 2014b. Petrogenesis of Late Cretaceous I-type granites in the southern Yidun Terrane: new constraints on the Late Mesozoic tectonic evolution of the eastern Tibetan Plateau. *Lithos* 208–209, 202–219.
- Wang, R., Richards, J.P., Hou, Z.Q., Yang, Z.M., DuFrane, S.A., 2014. Increased magmatic water content – the key to Oligo-Miocene porphyry Cu–Mo±Au formation in the Eastern Gangdese Belt, Tibet. *Econ. Geol.* 109, 1315–1339.
- Weislogel, A.L., 2008. Tectonostratigraphic and geochronologic constraints on evolution of the northeast Paleotethys from the Songpan-Ganzi complex, central China. *Tectonophysics* 451, 331–345.
- Xiao, L., Xu, Y.G., Xu, J.F., He, B., Pirajno, F., 2004. Chemostratigraphy of flood basalts in the Garze-Litang region and Zongza Block: implications for western extension of the Emeishan Large Igneous Province, SW China. *Acta Geol. Sin.* 78, 61–67.
- Xiao, L., Zhang, H.F., Clemens, J.D., Wang, Q.W., Kan, Z.Z., Wang, K.M., Ni, P.Z., Liu, X.M., 2007. Late Triassic granitoids of the eastern margin of the Tibetan Plateau: geochronology, petrogenesis and implications for tectonic evolution. *Lithos* 96, 436–452.
- Xu, X.W., Cai, X.P., Qu, W.J., Song, B.C., Qin, K.Z., Zhang, B.L., 2006. Later Cretaceous granitic porphyritic Cu–Mo mineralization system in the Hongshan area, northwestern Yunnan and its significances for tectonics. *Acta Geol. Sin.* 80, 1422–1433 (in Chinese with English abstract).
- Yang, Y.Q., Hou, Z.Q., Huang, D.H., Qu, X., 2002. Collision orogenic process and magmatic metallogenic system in Zhongdian island arc. *Acta Geosci. Sin.* 23, 17–24 (in Chinese with English abstract).
- Yang, F., Zou, G.F., Wu, J., Li, F., Jiang, Y.G., Zhao, X.D., 2011. Ages and geological significance of the porphyries in the Chundu copper mining area in Zhongdian, Yunnan province. *Geotect. Metall.* 35, 307–314 (in Chinese with English abstract).
- Yang, T.N., Hou, Z.Q., Wang, Y., Zhang, H.R., Wang, Z.L., 2012. Late Paleozoic to Early Mesozoic tectonic evolution of northeast Tibet: evidence from the Triassic composite western Jinsha-Garze–Litang suture. *Tectonics*. <http://dx.doi.org/10.1029/2011TC003044>.
- Yang, T.N., Ding, Y., Zhang, H.R., Fan, J.W., Liang, M.J., Wang, X.H., 2014. Two-phase subduction and subsequent collision defines the Paleotethyan tectonics of the southeastern Tibetan Plateau: evidence from zircon U–Pb dating, geochemistry, and structural geology of the Sanjiang orogenic belt, southwest China. *Geol. Soc. Am. Bull.* 126, 1654–1682.
- Yang, L.Q., Deng, J., Dilek, Y., Meng, J.Y., Gao, X., Santosh, M., Wang, D., Yan, H., 2015. Melt source and evolution of I-type granitoids in the SE Tibetan Plateau: Late Cretaceous magmatism and mineralization driven by collision-induced transtensional tectonics. *Lithos*. <http://dx.doi.org/10.1016/j.lithos.2015.10.005>.
- Yin, G.H., Li, W.C., Jiang, C.X., Li, J.K., Xu, D., Yang, S.R., 2009. The evolution of Relin uplex rock masses in Yanshan Phase and Ar–Ar dating age and copper-molybdenum mineralization characteristics of Zhongdian volcanic–magma arc. *Geol. Explor.* 45, 385–394 (in Chinese with English abstract).
- Zhang, X.C., Leng, C.B., Yang, C.Z., Wang, W.Q., Qin, C.J., 2009. Geochronology study of copper-mineralized Chundu porphyry intrusion, Zhongdian, SW Yunnan Province, China: SIMS U–Pb zircon age and its geological significance. *Acta Mineral. Sin.* 29, 359–360 (in Chinese).
- Zhao, Y.J., Yuan, C., Zhou, M.F., Yan, D.P., Long, X.P., Cai, K.D., 2007. Post-orogenic extension of Songpan-Garzê orogen in Early Jurassic: constraints from Niuxingou monzodiorite and Siguniangshan A-type granite of western Sichuan, China. *Geochemica* 36, 139–142 (in Chinese with English abstract).
- Zu, B., Xue, C.J., Zhao, Y., Qu, W.J., Li, C., Symons, D.T., Du, A.D., 2015. Late Cretaceous metallogeny in the Zhongdian area: constraints from Re–Os dating of molybdenite and pyrrhotite from the Hongshan Cu deposit, Yunnan, China. *Ore Geol. Rev.* 64, 1–12.